CIRP Annals - Manufacturing Technology 65 (2016) 373–376

Contents lists available at ScienceDirect

CIRP Annals - Manufacturing Technology

journal homepage: http://ees.elsevier.com/cirp/default.asp

A trajectory optimization method for improved tracking of motion commands using CNC machines that experience unwanted vibration

C. Okwudire *, K. Ramani, M. Duan

Mechatronics and Sustainability Research Laboratory, University of Michigan, Ann Arbor, USA
Submitted by T. Hoshi (1), Toyohashi, Japan

ARTICLE INFO

Keywords:
Computer numerical control (CNC)
Vibration
Trajectory optimization

ABSTRACT

This paper presents a trajectory optimization method for minimizing tracking errors in CNC machines that experience unwanted vibration. The motion command sent to the machine is parameterized using B-splines whose basis functions are filtered using a model of the machine's dynamics. The control points associated with the filtered basis functions are then selected to minimize tracking errors subject to the kinematic limits of the machine. The proposed method is shown to be very systematic and easy to use, and it does not sacrifice tracking speed. Experiments are used to demonstrate its superior performance compared to an existing method.

1. Introduction

Computer numerical control (CNC) powered feed drives are used for generating motion in a wide range of manufacturing machines, e.g., machine tools, laser cutters and 3D printers. Therefore, their speed and accuracy are critical to the quality and productivity of the associated manufacturing machines and processes [1]. Tracking and contouring performance are two metrics commonly used to quantify the accuracy of CNC feed drives [2]. Tracking accuracy refers to how well the actual position of a feed drive follows a desired trajectory, while contouring accuracy is a measure of how close the actual position keeps to a desired motion path [2]. Most CNC feed drives achieve good tracking accuracy (directly) and contouring accuracy (indirectly) by minimizing axis tracking errors [2]. Therefore, this paper focuses on improving axis tracking accuracy, assuming that contouring accuracy is also indirectly enhanced.

It is not uncommon for a CNC-driven machine to have one or more unwanted vibration modes, arising from structural flexibilities of its mechanical components. For example, vibration modes could stem from ball screws, machine columns/beds, or even from fixtures added to a machine. Such unwanted vibration modes are often excited by motion commands sent to the CNC machine, resulting in degradation of tracking accuracy.

One approach to reduce the loss of tracking accuracy caused by motion commands is to suppress the resulting vibration of the machine using feedback controllers [3,4]. However, the presence of vibration modes often introduces stability concerns in feedback loops, especially when sensors and actuators are non-collocated [3]. Another approach is to use vibration suppression devices [5–7], requiring that the machine be furnished with extra hardware, which may not be practical nor desirable.

An alternative approach, that does not require extra hardware nor incur stability issues, is to generate the motion commands sent to the CNC such that unwanted vibration is avoided or reduced. The most popular approach for achieving this goal is to generate motion commands that are smooth (i.e., commands that have little or no high-frequency content) [1]. However, the attenuated high-frequency content of smooth motion commands often implies loss of motion speed, which adversely affects productivity [1]. Another problem with smooth motion commands is that, because they are not generated using knowledge of the machine's dynamics, they often yield suboptimal vibration reduction [8]. Better vibration reduction can be achieved by using filters (e.g., FIR filters) or input shapers [8–10] to generate motion commands with low frequency content around the resonance modes of the machine (assuming that its dynamics is known). However, filters and input shapers introduce time delays which sacrifice productivity and could severely degrade tracking and contouring accuracy [8–10].

Altintas and Khoshdarregi [9] demonstrated a method for reducing input-shaper-induced contour errors by predicting and compensating for the errors via modifications to the motion commands sent to the machine. However, their method cannot guarantee the minimization of errors, nor can it ensure that kinematic constraints imposed on the motion trajectory are not violated. Moreover, it does not eliminate the loss of motion speed caused by the delays of the input shaper.

This paper presents a trajectory optimization method that minimizes tracking errors in CNC machines that have unwanted vibration modes. The interpolated motion commands sent to the machine are parameterized using B-splines whose basis functions are filtered using a model of the machine's dynamics. The control points associated with the filtered basis functions are then selected to minimize tracking errors while satisfying the kinematic limits of the machine. The proposed method is shown to be very systematic and easy to use, and it does not sacrifice tracking speed. Section 2

* Corresponding author.
E-mail address: okwudire@umich.edu (C. Okwudire).

http://dx.doi.org/10.1016/j.cirp.2016.04.100
0007-8506/© 2016 CIRP.

describes the method, while Section 3 presents experimental results that demonstrate its superior tracking and contouring performance compared to Altintas and Khoshdarregi's [9] approach. Conclusions and future work are presented in Section 4.

2. Proposed trajectory optimization method

Fig. 1 shows the dynamics ($G(s)$) of a CNC feed drive axis, including its unwanted vibration modes, given by the transfer function

Fig. 1. Dynamics G of a CNC feed axis including unwanted vibration modes.

$$G(s) = \sum_{i=1}^{M} \frac{\alpha_i + \beta_i s}{s^2 + 2\zeta_i \omega_{n,i} s + \omega_{n,i}^2} \tag{1}$$

where M represents the number of modes, while α_i and β_i are the residue constants, ζ_i is the damping ratio and $\omega_{n,i}$ is the natural frequency of the i^{th} mode in rad/s. It is desired to generate x_{dm}^*, a modified and optimized version of desired position trajectory x_d, such that, when applied to the feed axis in place of x_d, minimizes the tracking errors caused by G while satisfying the kinematic limits of the machine axis.

Fig. 2 shows a block diagram of the proposed approach for generating x_{dm}^*; it is based on the concept of filtered basis functions previously introduced by the authors in the context of tracking control of non-minimum phase systems [11]. Let $\boldsymbol{x}_d = [x_d(0)\; x_d(1)\; \ldots\; x_d(E)]^T$ represent $E + 1$ discrete time steps of the x-component of a toolpath interpolated by a CNC (i.e., the desired trajectory). We assume that the CNC has look ahead capabilities such that the $E + 1$ time steps of $\boldsymbol{x}_d$ are known in advance. Furthermore, we assume that the modified but un-optimized motion command, $\boldsymbol{x}_{dm} = [x_{dm}(0)\; x_{dm}(1)\; \ldots\; x_{dm}(E)]^T$, is parameterized in the CNC using B-splines such that

$$\underbrace{\begin{bmatrix} x_{dm}(0) \\ x_{dm}(1) \\ \vdots \\ x_{dm}(E) \end{bmatrix}}_{\boldsymbol{x}_{dm}} = \underbrace{\begin{bmatrix} N_{0,m}(\xi_0) & N_{1,m}(\xi_0) & \cdots & N_{n,m}(\xi_0) \\ N_{0,m}(\xi_1) & N_{1,m}(\xi_1) & \cdots & N_{n,m}(\xi_1) \\ \vdots & \vdots & \ddots & \vdots \\ N_{0,m}(\xi_E) & N_{1,m}(\xi_E) & \cdots & N_{n,m}(\xi_E) \end{bmatrix}}_{\boldsymbol{N}} \underbrace{\begin{bmatrix} p_0 \\ p_1 \\ \vdots \\ p_n \end{bmatrix}}_{\boldsymbol{p}} \tag{2}$$

For a B-spline of degree m, having $n + 1 \le E + 1$ control points, $p_0, p_1, \ldots, p_n$, and knot vector, $[g_0\, g_1 \ldots g_{m+n+1}]^T$, $N_{j,m}(\xi)$ are real-valued basis functions given by [11,12]

$$\begin{aligned} N_{j,m}(\xi) &= \frac{\xi - g_j}{g_{j+m} - g_j} N_{j,m-1}(\xi) + \frac{g_{j+m+1} - \xi}{g_{j+m+1} - g_{j+1}} N_{j+1,m-1}(\xi) \\ N_{j,0}(\xi) &= \begin{cases} 1 & g_j \le \xi < g_{j+1} \\ 0 & \text{otherwise} \end{cases} \end{aligned} \tag{3}$$

where $j = 0, 1, \ldots, n$ and $\xi \in [0, 1]$ is the spline parameter, representing normalized time, which is discretized in Eq. (2) into $E + 1$ uniformly spaced points, $\xi_0, \xi_1, \ldots, \xi_E$. Without loss of generality, the knot vector is selected to be uniform, such that

$$g_k = \begin{cases} 0 & 0 \le k \le m \\ \dfrac{k - m}{n - m + 1} & m + 1 \le k \le n \\ 1 & n + 1 \le k \le m + n + 1 \end{cases} \tag{4}$$

Notice that if $\boldsymbol{x}_{dm}$ given in Eq. (2) is applied as the motion command to the CNC feed axis of Fig. 1, in place of $\boldsymbol{x}_d$, the control point vector, $\boldsymbol{p}$, is not affected by G, because $\boldsymbol{p}$ is not a function of time; however, the basis functions matrix, $\boldsymbol{N}$, which is a function of time, is filtered by G. Therefore, the resulting position $\boldsymbol{x} = [x(0)\; x(1)\; \ldots\; x(E)]^T$ can be approximated by

$$\boldsymbol{x} \approx \tilde{\boldsymbol{N}}\boldsymbol{p} \tag{5}$$

$$\boldsymbol{e} = \boldsymbol{x}_d - \boldsymbol{x} \approx \boldsymbol{x}_d - \tilde{\boldsymbol{N}}\boldsymbol{p} \tag{6}$$

One useful mathematical property of B-splines is that the derivative of a B-spline curve is also a B-spline curve that can be expressed linearly in terms of the control points of the original curve. Hence, the r^{th} derivative of $\boldsymbol{x}_{dm}$ can be written as [11]

$$\frac{d^r \boldsymbol{x}_{dm}}{dt^r} = \boldsymbol{N}_r \boldsymbol{p} \tag{7}$$

where $\boldsymbol{N}_r$ is the basis function matrix for the r^{th} derivative of position; its elements can be calculated readily from those of $\boldsymbol{N}$ [11,12]. Therefore, to achieve the stated objective of this paper, $\boldsymbol{x}_{dm}^* = \boldsymbol{N}\boldsymbol{p}^*$ can be generated using optimal control points, $\boldsymbol{p}^*$, calculated to minimize the objective function given by

$$\begin{aligned} &\boldsymbol{p}^* = \arg\min_{\boldsymbol{p}} (\boldsymbol{e}^T\boldsymbol{e}) \approx \arg\min_{\boldsymbol{p}} ((\boldsymbol{x}_d - \tilde{\boldsymbol{N}}\boldsymbol{p})^T (\boldsymbol{x}_d - \tilde{\boldsymbol{N}}\boldsymbol{p})) \\ &\text{s.t.} \quad \|\boldsymbol{N}_r \boldsymbol{p}\|_\infty \le L_r \end{aligned} \tag{8}$$

where L_r represents the kinematic limit associated with the r^{th} derivative of $\boldsymbol{x}_{dm}$ (e.g., its velocity, acceleration and jerk limits), while $\|\cdot\|_\infty$ denotes the infinity norm (i.e., the maximum absolute value of the elements) of a vector.

Notice that, if the kinematic constraints are not considered, the solution to Eq. (8) reduces to a traditional least-squares fitting problem [11] where

$$\boldsymbol{p}^* = ((\tilde{\boldsymbol{N}}^T\tilde{\boldsymbol{N}})^{-1}\tilde{\boldsymbol{N}}^T)\boldsymbol{x}_d \tag{9}$$

However, with the constraints included, Eq. (8) becomes a least squares problem with inequality constraints, which has a guaranteed solution as long as the constraints are feasible. The solution is unique if the matrix $\tilde{\boldsymbol{N}}$ is full rank (i.e., if the filtered basis functions are linearly independent [11]). The authors have shown in their previous work [11] that linear dependence of the filtered basis functions is highly improbable. The proposed method achieves trajectory parameterization, constraint enforcement and optimization simultaneously using industry-standard B-splines and basic least squares techniques, making it easy to use. Notice also that both $\boldsymbol{x}_d$ and $\boldsymbol{x}_{dm}^*$ have the same length (i.e., $E + 1$), meaning that the proposed method does not sacrifice motion speed. Though the method has been discussed for a single axis (i.e., x), it is readily applicable to multiple axes of a CNC machine by treating each axis separately; therefore, it is very systematic and scalable.

3. Experimental validation

Experimental results are presented in this section to compare the proposed technique to the input shaping with contour error compensation (i.e., IS + CEC) technique proposed by Altintas and Khoshdarregi [9]. The biaxial (X–Y) linear motor driven stage (Aerotech ALS 25010) shown in Fig. 3 is used for the experiments.

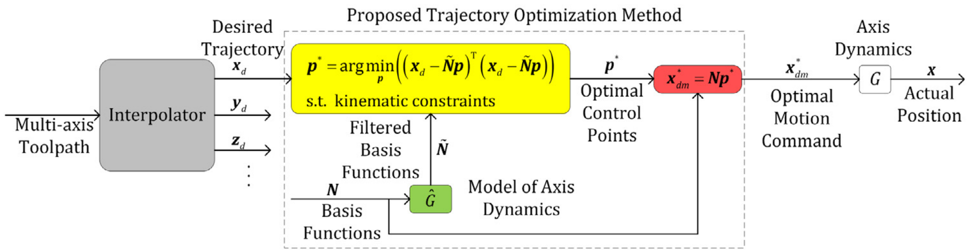

Fig. 2. Block diagram of the proposed trajectory optimization method (applied to the x-component of a multi-axis toolpath).

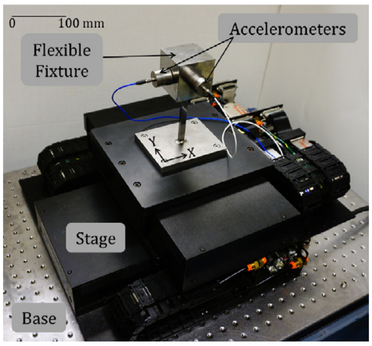

Fig. 3. Experimental setup – biaxial stage with flexible fixture.

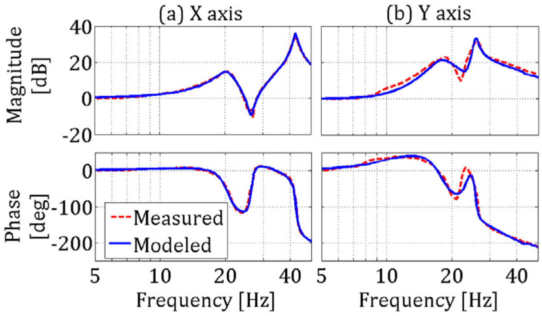

Fig. 4. Measured and modeled frequency response functions of X and Y axes of experimental set up.

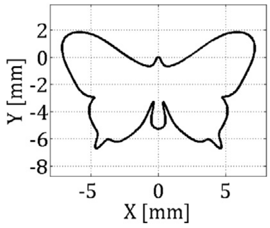

Fig. 5. Desired path.

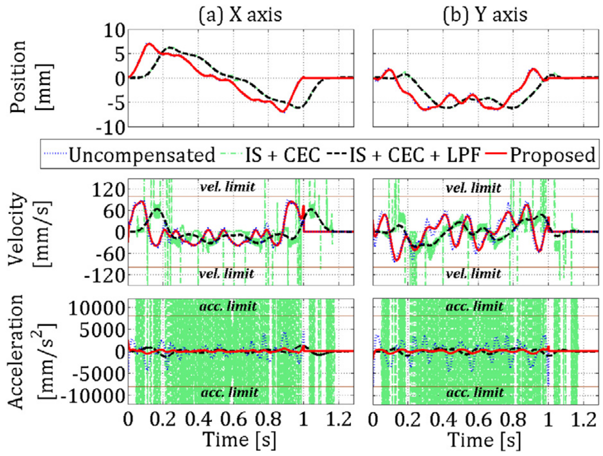

Fig. 6. X and Y axis command signals for uncompensated, IS + CEC (without LPF), IS + CEC + LPF and proposed (optimal) trajectories.

The stage is controlled using a traditional P/PI feedback controller, augmented with velocity and acceleration feedforward [13]. The controller is implemented on a dSPACE 1103 real-time control board with 10 kHz sampling frequency. The velocity and acceleration limits for both of its axes are L_1 = 100 mm/s and L_2 = 8000 mm/s^2, respectively. As shown in the Fig. 3, the stage is equipped with a fixture consisting of a block mounted on a rod. The block is assumed to represent an apparatus (e.g., a tool, workpiece or measurement device) whose x and y positions are expected to track their respective desired trajectories, x_d and y_d, accurately, in spite of inherent structural flexibilities. The acceleration of the fixture is measured using two unidirectional accelerometers (PCB Piezotronics 393B05) shown in Fig. 3.

Fig. 4 shows the frequency response function (FRF) of the dynamics G of each axis of the stage, generated by applying swept sine acceleration (i.e., $\ddot{x}_d$ and $\ddot{y}_d$) commands to the stage and measuring the corresponding accelerations of the fixture (i.e., $\ddot{x}$ and $\ddot{y}$) using the accelerometers. The dynamics of each axis exhibits two dominant modes, which are very obvious in Fig. 4.

For each axis, the lower mode is a mode from the stage while the higher mode is from the flexible fixture (whose natural frequencies are different in the x and y directions because the mounting rod has a rectangular cross section). However, not obvious in Fig. 4 are two much less dominant modes in each FRF. In other words, there are four unwanted modes (M = 4) in each axis' dynamics, whose parameters are identified using the rational fraction polynomial method [14], and are summarized in Table 1. Fig. 4 shows an excellent fit between the modeled and actual FRFs for the X-axis.

The model for the Y-axis is not as accurate as that of the X-axis because the two dominant modes of the Y axis are relatively more damped and closer in resonance frequency, making it harder to curve fit them [15]. However, the fitting errors of the Y axis provide an opportunity to test the performance of the proposed method in the presence of some modeling errors, which are likely to occur in practice.

Fig. 5 shows the butterfly curve used as the desired path for the experiments (see [16] for details). Fig. 6 shows the position trajectories, x_d and y_d, (i.e., the uncompensated motion commands) of the desired path, as well as its velocity and acceleration profiles, as functions of time. Notice that the duration of the desired trajectories is 1 s (i.e., $E = 10^4$, based on 10 kHz sampling frequency). The uncompensated trajectories are compared with the corresponding modified trajectories obtained from IS + CEC [9] and from the proposed method. The zero-vibration and derivative (ZVD) input shaper is used for the IS + CEC method. For each mode, the ZVD shaper consists of three impulses, A_1, A_2 and A_3, placed at times 0, 0.5T_d and T_d, respectively, as reported in Table 2 (where T_d is the vibration period) [9]. Note that the shapers for the X and Y axes are convolved so that both axes have the same shaper [9]. CEC is performed using the method presented by Yang and Altintas [17], which is superior to that presented by Altintas and Khoshdarregi [9]. Notice from Fig. 6 that when IS + CEC is implemented without a low pass filter (LPF) applied to the modified motion commands, the axis velocity and acceleration limits are violated. This is because CEC introduces discontinuities

Table 1
Model parameters of vibration dynamics for X and Y axes of stage.

Axis-mode#	$\omega_{n,i}$ (Hz)	ζ_i	α_i	β_i
X-1	20.52	0.092	15,797.5	54.3
X-2	34.94	0.540	−135,160.6	−587.7
X-3	42.53	0.029	189,225.5	−60.5
X-4	42.60	0.007	14,633.4	−67.9
Y-1	17.86	0.120	6,709.0	310.4
Y-2	25.70	0.021	42,872.2	169.4
Y-3	30.66	0.440	−43,178.2	−1,260.2
Y-4	43.10	0.036	−966.3	7.5

Table 2
Input shaper parameters.

Axis-mode#	A_1	A_2	A_3	T_d
X-1	0.3273	0.4896	0.1831	0.0489
X-2	0.7787	0.2075	0.0138	0.0340
X-3	0.2733	0.4990	0.2277	0.0235
X-4	0.2554	0.4999	0.2446	0.0235
Y-1	0.3526	0.4824	0.1650	0.0564
Y-2	0.2668	0.4995	0.2338	0.0389
Y-3	0.6779	0.2909	0.0312	0.0363
Y-4	0.2791	0.4984	0.2225	0.0232

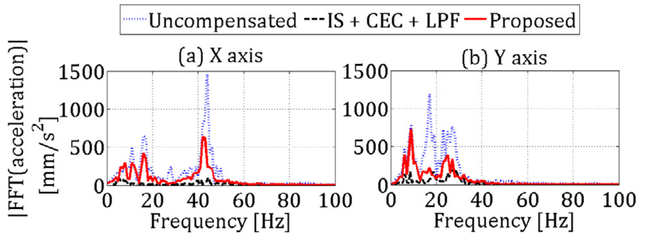

Fig. 7. Fast Fourier transform (FFT) of measured acceleration of fixture for uncompensated, IS + CEC + LPF and proposed (optimal) trajectories.

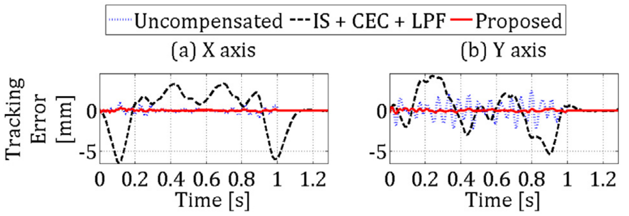

Fig. 8. X and Y axis position tracking errors for uncompensated, IS + CEC + LPF and proposed (optimal) trajectories.

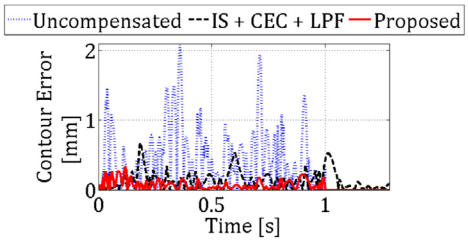

Fig. 9. Contour errors for uncompensated, IS + CEC + LPF and proposed (optimal) trajectories.

in the trajectory [9]. Observe also that the resultant trajectories last 0.2847 s (i.e., 28.47%) longer than their uncompensated counterparts, due to the delays introduced by the input shapers. To deal with the discontinuities, constraint violation and excitation of vibration modes due to CEC, a LPF with 3 Hz cut off frequency is applied to the signals generated by IS + CEC, as recommended in [9]. Note, however, that there is no guarantee that constraints will always be satisfied after applying a specific (e.g., 3 Hz) LPF; the effect of the LPF would vary depending on the given trajectory, therefore some iteration may be required. The proposed method is executed with B-splines of order $m = 5$, having $n + 1 = 51$ control points. Notice from Fig. 6 that the modified trajectories generated by the proposed method automatically satisfy the imposed kinematic constraints and do not have any delays (i.e., they last exactly as long as the desired trajectories).

The position trajectories from the uncompensated, IS + CEC + LPF and the proposed methods are applied to the X and Y axes of the stage as motion commands; the IS + CEC trajectory without LPF is not used in experiments because of its constraint violations. Fig. 7 shows the fast Fourier transform (FFT) of $\ddot{x}$ and $\ddot{y}$ (measured using the accelerometers) for the three methods. The X-axis acceleration energy spectral densities are 6.38×10^6 mm^2/s^4, 6.39×10^4 mm^2/s^4 and 1.92×10^6 mm^2/s^4, while the Y-axis acceleration energy spectral densities are 7.32×10^6 mm^2/s^4, 3.31×10^5 mm^2/s^4 and 1.81×10^6 mm^2/s^4 for the uncompensated, IS + CEC + LPF and the proposed methods, respectively. This means that the proposed method generates less vibration than the uncompensated; however, IS + CEC + LPF provides the smallest level of vibration because input shaping is focused on elimination of vibration while the proposed method focuses on accurate tracking – which are not exactly the same objective. To demonstrate this fact, the tracking errors, $x_d - x$ and $y_d - y$, for all three cases are plotted in Fig. 8, based on position signals (x and y) derived from the measured acceleration signals using an observer. The X-axis RMS tracking errors are 0.3014 mm, 2.5595 mm and 0.0852 mm, while the Y-axis RMS tracking errors are 1.0165 mm, 2.1709 mm and 0.1198 mm for the uncompensated, IS + CEC + LPF and the proposed methods, respectively. Fig. 9 compares the contour errors of the three methods. Their RMS values are 0.5508 mm, 0.1852 mm and 0.0880 mm for the uncompensated, IS + CEC + LPF and the proposed methods, respectively, indicating the ability of the proposed method to indirectly reduce contour errors via minimizing tracking errors. The implication is that the proposed method does better than IS + CEC + LPF in terms of the primary objective of improving tracking and contouring accuracy, even if it means allowing a little more vibration.

4. Conclusion

This paper has presented a systematic, scalable and easy to use trajectory optimization method that minimizes tracking errors in CNC machines that have unwanted vibration modes. The proposed method parameterizes the motion command to the machine as a linear combination of B-spline basis functions, which are then forward filtered using a model of the machine's dynamics. The associated control points are computed such that tracking errors are minimized while ensuring that axis kinematic constraints are not violated. The proposed method is compared in experiments to an input shaping and contour error compensation method, and is shown to yield significantly improved tracking and contouring accuracy, without loss of productivity.

Acknowledgements

The authors would like to thank Mr. Deokkyun Yoon for his assistance with the experimental setup presented in this paper. They would also like to thank Professor Hoshi for his constructive feedback. This work is partially funded by the National Science Foundation's CAREER Award #1350202.

References

[1] Altintas Y, Verl A, Brecher C, Uriarte L, Pritschow G (2011) Machine Tool Feed Drives. *Annals of the CIRP* 60(2):779–796.
[2] Erkorkmaz K, Altintas Y (2001) High Speed CNC System Design. Part III: High Speed Tracking and Contouring Control of Feed Drives. *International Journal of Machine Tools and Manufacture* 41(11):1637–1658.
[3] Kamalzadeh A, Erkorkmaz K (2007) Compensation of Axial Vibrations in Ball Screw Drives. *Annals of the CIRP* 56(1):373–378.
[4] Symens W, van Brussel H, Swevers J (2004) Gain-scheduling Control of Machine Tools with Varying Structural Flexibility. *Annals of the CIRP* 53(1):321–324.
[5] Ast A, Braun S, Eberhard P, Heisel U (2007) Adaptronic Vibration Damping for Machine Tools. *Annals of the CIRP* 56(1):379–382.
[6] Yoon D, Okwudire CE (2015) Magnet Assisted Stage for Vibration and Heat Reduction in Wafer Scanning. *Annals of the CIRP* 64(1):381–384.
[7] Verl A, Frey S (2012) Improvement of Feed Drive Dynamics by Means of Semi-active Damping. *Annals of the CIRP* 61(1):351–354.
[8] Singer N, Singhose W, Seering W (1999) Comparison of Filtering Methods for Reducing Residual Vibration. *European Journal of Control* 5(2):208–218.
[9] Altintas Y, Khoshdarregi MR (2012) Contour Error Control of CNC Machine Tools with Vibration Avoidance. *Annals of the CIRP* 61(1):335–338.
[10] Sencer B, Ishizaki K, Shamoto E (2015) High Speed Cornering Strategy with Confined Contour Error and Vibration Suppression for CNC Machine Tools. *Annals of the CIRP* 64:369–372.
[11] Duan M, Ramani KS, Okwudire CE (2015) Tracking Control of Non-minimum Phase Systems Using Filtered Basis Functions: A NURBS-based Approach. *Presented at the ASME 2015 Dynamic Systems and Control Conference (DSCC 2015).*
[12] Duan M, Okwudire C (2015) Minimum-time Cornering for CNC Machines Using an Optimal Control Method with NURBS Parameterization. *The International Journal of Advanced Manufacturing Technology* 1–14.
[13] Altintas Y, Okwudire CE (2009) Dynamic Stiffness Enhancement of Direct-driven Machine Tools Using Sliding Mode Control with Disturbance Recovery. *Annals of the CIRP* 58(1):335–338.
[14] Richardson M, Formenti D (1982) Parameter Estimation from Frequency Response Measurements Using Rational Fraction Polynomials. *Proceedings of the International Modal Analysis Conference*, 167–182.
[15] Tan J-B, Liu Y, Wang L, Yang WG (2008) Identification of Modal Parameters of a System with High Damping and Closely Spaced Modes by Combining Continuous Wavelet Transform with Pattern Search. *Mechanical Systems and Signal Processing* 22(5):1055–1060.
[16] Yang S, Ghasemi AH, Lu X, Okwudire CE (2015) Pre-compensation of Servo Contour Errors Using a Model Predictive Control Framework. *International Journal of Machine Tools and Manufacture* 98:50–60.
[17] Yang J, Altintas Y (2015) A Generalized On-line Estimation and Control of Five-axis Contouring Errors of CNC Machine Tools. *International Journal of Machine Tools and Manufacture* 88:9–23.